Simulations of water isotope abundances in the upper troposphere and lower stratosphere and implications for stratosphere troposphere exchange

Andrew Gettelman
National Center for Atmospheric Research, Boulder, Colorado, USA

Christopher R. Webster
Earth and Space Sciences Division, Jet Propulsion Laboratory, California Institute of Technology, Pasadena, California, USA

Received 24 March 2004; revised 25 February 2005; accepted 13 June 2005; published 8 September 2005.

[1] An analytic model of transport and microphysics in the tropical tropopause layer (TTL) is extended to include stable isotopes of water. The model, running along trajectories, is tested against in situ and satellite observations of HDO and $H_2^{18}O$ in the Upper Troposphere and Lower Stratosphere (UT/LS). The model is able to reproduce the range of isotopic depletions observed in the data, and reproduce individual episodes that mirror or depart from Rayleigh fractionation processes. The results indicate that water substance in the upper troposphere does not follow a Rayleigh distillation model due to the presence of condensed phase water. Stratospheric abundances of stable isotopes of water can be understood based on known isotopic physics, convective transport of ice, and gradual dehydration.

Citation: Gettelman, A., and C. R. Webster (2005), Simulations of water isotope abundances in the upper troposphere and lower stratosphere and implications for stratosphere troposphere exchange, *J. Geophys. Res.*, *110*, D17301, doi:10.1029/2004JD004812.

1. Introduction

[2] Stratospheric humidity has important implications for stratospheric ozone chemistry as well as for the radiation balance and climate of the upper troposphere and lower stratosphere (UT/LS). It is broadly known that most of the air and humidity enters the stratosphere in the tropics [*Brewer*, 1949; *Holton et al.*, 1995], but the details of how air and humidity enter the stratosphere are not well known [*Stratospheric Processes and their Role in Climate* (*SPARC*), 2000; *Rosenlof*, 2003]. Stratospheric humidity has likely increased significantly over the past century as methane concentrations have increased in the atmosphere, but there are additional interannual variations in the water vapor content of the stratosphere which are not fully understood [*Randel et al.*, 2003; *SPARC*, 2000]. Stable isotopes of water (''isotopes'') provide important additional constraints on the atmospheric hydrologic budget. The heavier isotopes of water (HDO and $H_2^{18}O$ being the most common after $H_2^{16}O$) have slightly lower vapor pressures than $H_2^{16}O$ (hereafter just H_2O). The result is that these species preferentially exist in the condensed phase, and the ratio of an isotope to its parent R (in atmospheric water vapor) is depleted relative to the ratio in standard mean ocean water (R_0). Depletion provides an integrated history of condensation and evaporation. Depletion is measured in parts per thousand (per mil) using the standard δ notation, where for isotope X, $\delta X \equiv 1000\ (R/R_o - 1)$. Thus an air parcel with 65.3% of its HDO removed would be described by $\delta D = -653$ per mil.

[3] Some of the first isotopic measurements of water in the upper troposphere were made by [*Ehhalt*, 1974]. An updated version of data from [*Ehhalt*, 1974] indicates a mean annual HDO depletion in the upper troposphere at 9 km over Nebraska (41°N) of $\delta D = -423$ per mil, with a standard deviation of around 70 per mil (D. H. Ehhalt, personal communication, 2004). Subsequent authors have noted that the stratosphere is ''underdepleted'' relative to a Rayleigh distillation model, which removes isotopically enriched condensate as soon as it is formed. In this work we define the ''Rayleigh'' curve as being simple distillation at 100% relative humidity along a temperature profile from the surface, assumed to be a moist adiabat.

[4] The estimated stratospheric entry depletion (δD) is -653 per mil [*McCarthy et al.*, 2004]. Similar values have been observed using Atmospheric Trace Molecule Spectroscopy (ATMOS) instrument data from the space shuttle [*Moyer et al.*, 1996; *Kuang et al.*, 2003; *Ridal*, 2002] and FIRS balloon observations [*Johnson et al.*, 2001b]. *Moyer et al.* [1996] first noted that the ''underdepletion'' requires lofting of isotopically heavier ice which subsequently evaporates. *Keith* [2000] noted that stratospheric isotopic ratios are not consistent with a simple model of isotopic physics (see below). *Johnson et al.* [2001b] and *Kuang et al.* [2003] have invoked theories to explain the observed distribution whereby convection dilutes water vapor by creating and mixing relatively dry air. This dilution process has recently been

0148-0227/05/2004JD004812$09.00

simulated by *Dessler and Sherwood* [2003] and compared to the ATMOS data, producing near-uniform depletion in the tropics.

[5] Here we extend an alternative model of dehydration and transport in the UT/LS and the Tropical Tropopause Layer (TTL) to include isotopes and compare it to recently available observations of water and its isotopes from aircraft [*Webster and Heymsfield*, 2003] and the space shuttle [*Kuang et al.*, 2003]. The model is able to reproduce the wide range of δD and $\delta^{18}O$ in the observations, largely due to substantial transport of water as condensate (ice). The model results and observations illustrate that we should not expect the UT/LS to lie near a single Rayleigh curve from the surface to the upper troposphere, if evaporated condensate is a significant portion of the hydrologic budget of the upper troposphere. We also use the results to discuss transport of air into the stratosphere and show that the physics of isotopes is consistent with final dehydration of air through fractionation under supersaturated conditions in cirrus clouds, as well as with dilution through mixing with dehydrated stratospheric air through isentropic and/or convective mixing.

[6] In section 2 we describe methods, the model and the data, in section 3 we present results from the simulations compared to observations. Section 4 discusses these results focusing on TTL transport, and conclusions are summarized in section 5.

2. Methodology

[7] We use data, as described below, from the UT/LS region. We will also specifically focus on air with characteristics of the Tropical Topopause Layer (TTL). We define the TTL following *Gettelman and Forster* [2002] as the layer between the level of maximum convective outflow and the cold point tropopause. Practically, this ranges vertically between the 345 K and the 400 K potential temperature surfaces ($\sim$13–18 km altitude). This definition does not have a meridonal boundary but is basically found equatorward of the subtropical jets. In order to further separate tropical or tropically influenced air from extratropical air, we use chemical tracers in addition to an altitude and potential temperature range. We use both the absence of a stratospheric tracer (ozone) and the presence of two tropospheric tracers (carbon monoxide and methane) to exclude aged extratropical stratospheric air. We require tropical or TTL air to have an ozone concentration [O_3] < 150 ppbv (parts per billion by volume), a carbon monoxide concentration [CO] > 40 ppbv and a methane concentration [CH_4] > 1800 ppbv. These definitions are taken in part from extratopical in situ aicraft CO and O_3 data [*Hoor et al.*, 2004] and satellite O_3 data [*Gettelman et al.*, 2004b]. This is similar to the approach using reactive nitrogen (NO_y) by [*Webster and Heymsfield*, 2003], and it restricts "TTL air" to parcels that have chemical signatures of the tropics (low ozone, high carbon monoxide, and high methane). For this description of TTL air, even if this air is found above the local tropopause, it may be chemically characteristic of tropical, not extratropical air. The results presented for the TTL are not acutely sensitive to the threshold values chosen, and definitions based on NO_y and CH_4 also yield a similar set of points.

[8] The key point here is not that we can unambiguously determine all air mass origins but that the air is in a region which has thermodynamic characteristics of the TTL (separation between the maximum convective outflow and the tropopause), and it does not have the chemical signature of aged stratospheric air, but rather of recently tropospheric air.

2.1. Data

[9] In this study we will compare simulations of water and its isotopes to data taken during the Cirrus Regional Study of Tropical Anvils and Cirrus Layers - Florida Area Cirrus Experiment (CRYSTAL-FACE). A complete overview of the mission, instruments, and data is available at http://cloud1.arc.nasa.gov/crystalface/. We focus on in situ observations in the Upper Troposphere and Lower Stratosphere taken from the NASA WB-57 aircraft based in Key West, Florida.

[10] Key West is on the edge of the tropics (24.5°N latitude), and in the summer season has conditions typical of the tropics in the UT/LS. In order to verify that this air is characteristic of the tropics, we have examined radiosonde soundings taken during the campaign from several stations (including Key West, Miami, Tampa Bay, and mobile sites). We find that there is a "TTL" in this region from 10–12 km (the minimum lapse rate) to $\sim$16 km (the cold point tropopause). In addition, ozone begins to increase above 12 km, also characteristic of the TTL [*Folkins et al.*, 1999]. On the basis of the criteria above for separating tropical from extratropical air, nearly 50% of the points at flight altitudes sampled "tropical" or tropospheric air this region with thermodynamic characteristics of the TTL.

[11] In particular, we use observations of total water and isotopes from the ALIAS instrument [*Webster and Heymsfield*, 2003]. The accuracy of a single isotopic ratio measurement from ALIAS is approximately ±50 per mil for δD in HDO and $\delta^{18}O$ in $H_2^{18}O$, with larger uncertainty for [H_2O] < 10 ppmv (parts per million by volume). To further verify the self-consistency of the ALIAS data, we have examined the correlation δD v. $\delta^{18}O$ (not shown) and found a slope similar to observations. At low depletions (higher temperatures) the slope is similar to the observed "meteoric water line" ($\delta D = 8 \times \delta^{18}O$), with scatter on the order of ±50 per mil. At larger depletions ($\delta D < -500$), $\delta^{18}O$ is larger than this relation would suggest. This deviation could be due to the increased uncertainty at lower total water mixing ratios, to a systematic error, or to kinetic effects causing deviations from the expected relationship.

[12] In addition, we use observations from two other instruments on the same aircraft developed at Harvard University for total water and water vapor [*Weinstock et al.*, 1994]. The quoted uncertainty for these instruments is ±5%. These two instruments for water vapor and total water are used to derive ice water content (IWC) as total water minus water vapor, and separate clear from cloudy parcels. Similar results are obtained if particle data from the CAPS instrument [*Baumgardner et al.*, 2001] are used to classify clear and cloudy air. We also test the model against retrievals of HDO from the ATMOS experiment in 1994

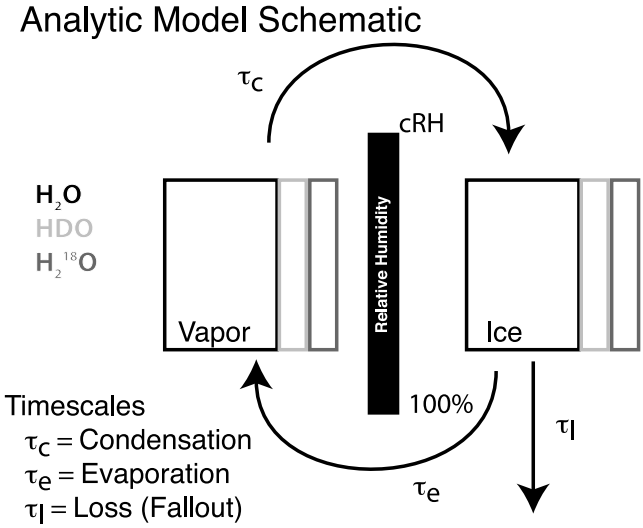

Figure 1. Schematic diagram of analytic microphysical model run along trajectories (see text for details).

[*Kuang et al.*, 2003] in the tropics. ATMOS has uncertainties of ±25 per mil HDO.

2.2. Model

[13] To simulate the data, we use an analytic microphysical model along trajectories described by *Gettelman et al.* [2002]. The model runs along back trajectories, using temperature and pressure to determine the bulk partitioning between vapor and ice. The model is illustrated schematically in Figure 1. At each time step the relative humidity (RH) is determined (with respect to either ice or liquid, depending on temperature). If the relative humidity is greater than a critical relative humidity threshold (cRH, typically 110%) then some vapor condenses with an *e*-folding time of τ_c. If RH < 100% then ice evaporates with an *e*-folding time of τ_e, and if there is any ice left, some falls out with an *e*-folding time of τ_l, which is a function of the ice water content. More ice corresponds to smaller τ_l (faster fallout). The model has been shown by *Gettelman et al.* [2002] to successfully reproduce the distribution of water vapor and ice in the TTL, given winds and temperatures.

[14] Model parameters remain largely unchanged from *Gettelman et al.* [2002], with a few exceptions. Stochastic temperature variations have been turned off for these simulations. The time for ice to sediment has been increased (decreased τ_l) by order of magnitude to enhance the quantity of ice. The timescales are still within the range discussed by *Heymsfield* [2003]. This last change makes the most significant difference, and was done so that the observed quantity of ice was closer to the quantity of ice from observations.

[15] The model has been modified to carry isotopes of H_2O (HDO and $H_2^{18}O$) and to perform the physics of fractionation upon condensation and evaporation. The model includes temperature dependent equilibrium (liquid) and nonequilibrium (ice) formulations for fractionation. Fractionation factors are taken from *Johnson et al.* [2001b] and are modified to reflect supersaturated conditions in the model according to [*Jouzel and Merlivat*, 1984] using the updated diffusivity ratios for HDO and $H_2^{18}O$ derived by *Cappa et al.* [2003]. Ice evaporation is treated as a last-in, first-out process, where the isotopic ratio evaporating is equal to the last isotopic ratio deposited. The sensitivity to this process is tested in section 3.1.

[16] Trajectories used to drive the model were derived from daily three-dimensional (3-D) ECMWF winds and temperatures. Back trajectories were calculated for 10 days, and output saved hourly. Data every 6 hours were used as input into the model. Trajectories were calculated running backward from points 1 min apart along each flight track. Twenty-seven trajectories from each point were used, at ±0.5 deg in latitude and longitude and ±1 km in altitude. This provides a better spread of points for testing the sensitivity of the model. All 27 points are plotted at each time in Figures 5 and 6.

[17] Simulations require initializations at the beginning of each trajectory for water and its isotopes. Initialization differs for points in the troposphere and stratosphere. The stratosphere is defined as the region above 16 km between 30°S and 30°N and above 9 km poleward of 30° latitude. H_2O is initialized at RH = 50% in the troposphere, and at 4 ppmv in the stratosphere. Results are not strongly sensitive to these initial conditions. Isotopes are initialized using the isotopic depletion at the initial temperature along a Rayleigh fractionation curve from the surface in the troposphere, and with fixed values of isotopic depletion ±1 σ sampled from a Gaussian distribution in the stratosphere. These values are -650 ± 20 per mil for for δD in HDO and -180 ± 5 per mil for $\delta^{18}O$ in $H_2^{18}O$. Stratospheric values only deviate significantly from these amounts if the trajectory experiences significant dehydration along its path.

[18] The model is capable of reproducing many aspects of the observations, but its heavily parameterized nature is a limitation for appropriately simulating processes that occur on smaller scales than the input trajectory data, such as convection or gravity wave motions. The rising motion associated with convection is implicitly included in the model, to the extent that the three dimensional wind field driving the trajectories includes the motion and diabatic heating from the convective parameterization in a global analysis. Trajectories in the free troposphere rise several kilometers in 6–12 hours, indicating the presence of convective motion. Diagnosed vertical velocities are probably an order of magnitude weaker than the observations in convective updrafts. Nonetheless, the model is able to well represent the large-scale vertical motion and temperature changes associated with convection, even on an individual event basis, as illustrated in the next section.

3. Results

[19] Here we present results from the model compared to various observed data sets. First, we examine some additional sensitivity tests (section 3.1). Then we compare the model to ALIAS HDO data (section 3.2), ALIAS $H_2^{18}O$ data (section 3.3) and finally ATMOS HDO data (section 3.4).

3.1. Sensitivity

[20] Extensive sensitivity tests have been conducted with the model to understand what parameters affect the distribution of water substance as well as the fractionation. As a metric, we use the mean δD for vapor + ice in the layer from

Table 1. Average Water and Isotopes 14–16 km[a]

Metric	All Observations	All Model	TTL Observations	TTL Model
All points				
H_2O total, ppmv	29(90)	29(23)	35(45)	31(23)
H_2O vapor, ppmv	16(6)	20(7)	22(6)	19(4)
Fraction of ice	45%	32%	37%	35%
δD, per mil	−596(187)	−718(91)	−573(176)	−707(83)
$\delta^{18}O$, per mil	−157(39)	−115(23)	−143(41)	−115(24)
Ice (total > 8× vapor)				
H_2O ice, ppmv	414(408)	202(128)	278(215)	174(40)
δD, per mil	−211(168)	−322(62)	−103(112)	−341(21)
$\delta^{18}O$, per mil	−29(35)	−40(8)	−14(34)	−42(3)
Clear (total < 1.2× vapor)				
H_2O vapor, ppmv	16(6)	18(8)	22(6)	20(5)
δD, per mil	−630(156)	−775(58)	−609(150)	−762(52)
$\delta^{18}O$, per mil	−167(29)	−131(18)	−154(26)	−126(16)

[a]Standard deviations in parentheses.

14 to 16 km (Table 1). In the model, this is −718 per mil for the standard case. For a series of sensitivity tests on all major model parameters, time steps and several treatments of ice fallout, the range of mean δD for clear and cloudy points was fairly small at −710 to −730 per mil. For example, the impact of equilibration of isotopic composition within condensate (as opposed to the last in first out layering approach) was 3 per mil in the average. The range of total water averaged over 14–16 km was 28–33 ppmv.

[21] Water vapor and ice are more sensitive to various parameters, but have been discussed elsewhere [*Gettelman et al.*, 2002]. The quantity of ice is critical for being able to reproduce the observed isotopic depletion, and in order to simulate reasonable ice distributions for the given trajectories, the time for fallout has been lengthened. The timescale only matters for larger ice water contents typical of the UT/LS (tens to hundreds of ppmv). The model is not sensitive to the timescale for fallout of small ice water contents (because they contain little water substance).

3.2. Comparison to ALIAS HDO

[22] Figure 2 illustrates the ALIAS isotopic data for HDO (in parts per mil) and the corresponding probability distribution of points from the trajectory simulations. Note that Figure 2 plots HDO in total water (vapor and ice combined) the quantity measured by ALIAS. We have plotted the same

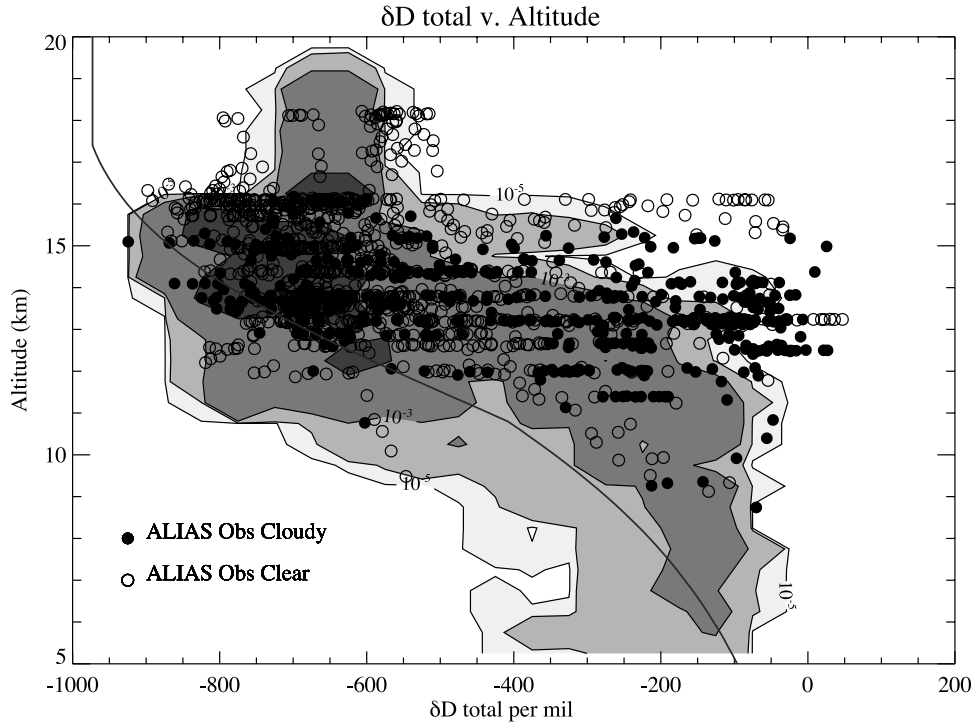

Figure 2. Depletion of HDO (δD) as a function of altitude. A binned PDF of simulated model results are shaded, and ALIAS observations are indicated for clear sky (open circles) and cloudy sky (closed circles). Cloudy sky is defined as total water greater than 120% of water vapor. A Rayleigh distillation curve from the surface is indicated as a solid line. Contour intervals for the PDF are 10^{-5}, 10^{-4}, 10^{-3}, and 10^{-2}.

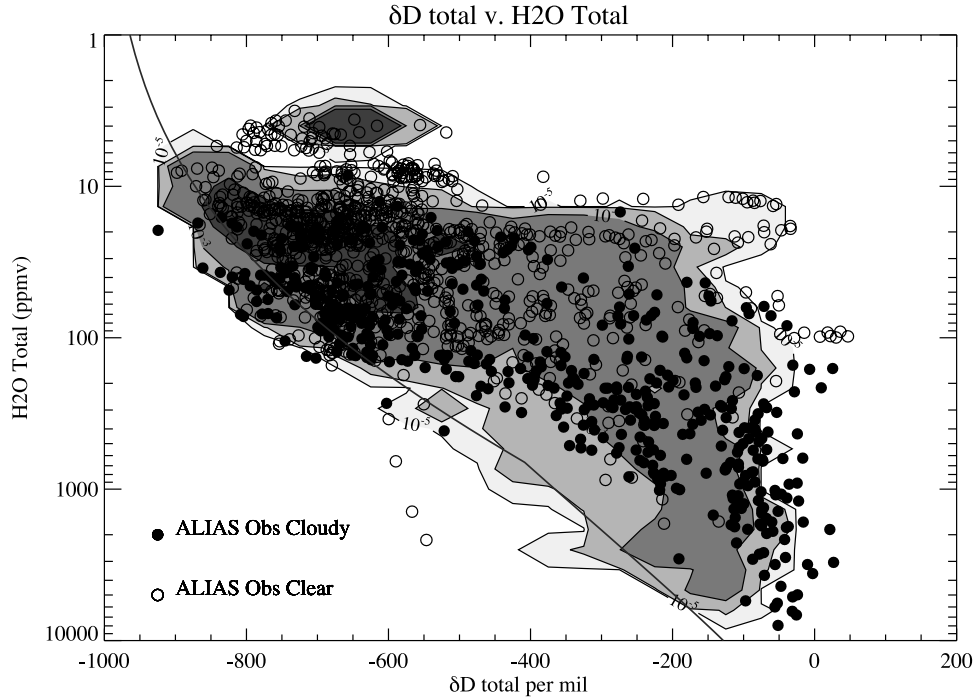

Figure 3. Same as for Figure 2, but depletion of HDO (δD) is shown as a function of total water mixing ratio (in ppmv).

quantity from the model, which tracks ice and vapor separately as a shaded probability distribution function (PDF) beneath the data.

[23] The model is able to simulate very well the envelope of the observations, with the exception of a few clear points at 16 km with very low depletion. The model was run with a threshold relative humidity for condensation of 110%. Figure 2 contains data from all nine CRYSTAL-FACE flights with isotopic data. If we select only those points where total water is in good agreement between ALIAS and the Harvard total water instrument (most of seven flights), we get similar results, indicating that the distributions and agreement are not dependent on the exact selection of data.

[24] Similar results are seen if the data are plotted as a function of water vapor rather than altitude (Figure 3). Note that there is a large range of observations of isotopic depletion even at low water concentrations in the UT/LS region sampled by ALIAS. Stated another way, for any given total water amount, there is a wide range of isotopic depletions. This is even true for low water vapor amounts in the UT/LS (the clear sky points in Figure 3). The model is able to simulate this variability.

[25] Figure 4 presents the same distribution as Figure 3, but limited to those points characteristic of the TTL based on altitude, potential temperature and chemical composition (low O_3, high CO, and high CH_4) as described in section 2. It is clear that the model solutions are valid in regions characteristic of the TTL as well. It does not matter how the data are plotted, the model is able to reproduce the observations of HDO in altitude or in total water concentration.

[26] The model, which contains all the standard isotopic physics, does not place the bulk of the observations on a Rayleigh curve, and has some points that are more depleted than a Rayleigh curve. These results are similar to the ALIAS observations. Maximum depletions, and the maximum variation of depletion are seen from 14 to 16 km, with an abrupt change in character at 16 km. The spread of observations in the stratosphere is related to tropopause height. Those points that are more depleted have a higher tropopause. A more compact relationship was found by *Webster and Heymsfield* [2003] when the data were sorted by height above the tropopause. The model depletion in the stratosphere is constrained by the initialization of the simulation. Those points that begin in the stratosphere are initialized with stratospheric water vapor and isotopic ratios of −650 per mil for HDO. The points are clearly seen as a discontinuous piece of the distribution in Figure 3. However, the location of the sharp transition in the model between a wide range of values in the troposphere, and a smaller range in the stratosphere (above the level of the tropical, not local tropopause), is fixed only by the climatological altitude of the tropical tropopause, indicating that the transition between tropospheric influenced air and mostly stratospheric air is well captured in both observations and in the simulation as the altitude of the tropical tropopause.

[27] We highlight statistics for the region from 14 to 16 km in Table 1. This layer is chosen as the most relevant for the stratosphere, since it is centered around the level of zero radiative heating in the tropics (∼15 km), above which air outside of convection begins to rise into the stratosphere [*Gettelman et al.*, 2004a]. The table presents results for all points, and just those with the isentropic location and chemical signature of tropical air ("TTL" air). In order to separate vapor from ice in the observations and model consistently, we have sorted the data by points where the ALIAS total water is less than 120% of the vapor measured by the Harvard water vapor instrument for clear sky, and where the total water measured by the

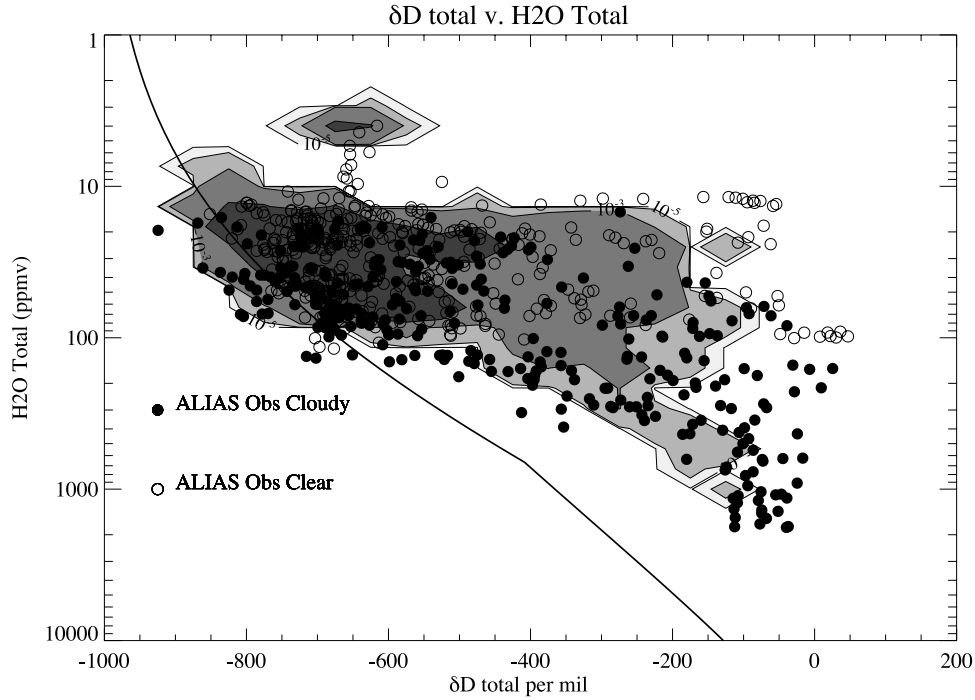

Figure 4. Same as for Figure 3, but depletion of HDO (δD) as a function of total water mixing ratio (in ppmv) from the model and observations is only shown for those points meeting the "TTL" criteria for O_3, CO, and CH_4 as described in the text.

Harvard total water instrument is greater than 8 times the measured vapor for cloudy sky. This is virtually identical to using the ice water content from the Harvard instruments. We separate clear from cloudy points in the model in the same way. Similar results are obtained if the analysis is repeated using the CAPS particle instrument ice water content (with a threshold of 2×10^{-3} g cm^{-3}, or $\sim$1 ppmv), though comparisons with the model are not as direct. The model has generally higher averaged depletion than the observations, though the distribution is well represented, as indicated in Figure 2. The mean of the model distribution for TTL air has less total water than the observations of TTL air, and in general the model has a smaller fraction of ice than the observations. Ice is enriched in heavy isotopes compared to the vapor in the model and observations. In general the air with tropical characteristics ("TTL" air) is similar to the overall distribution of points from CRYSTAL-FACE, as expected from the similarity of Figures 3 and 4.

[28] The model is able to reproduce the observations because it broadly simulates individual events along the flight tracks. As examples, we show samples of a convective event and a cirrus cloud event. For these two extreme cases the model is able to simulate the difference in water vapor, ice and isotopic depletion found in the observations. In nine flights, we do not see any cases in which the model and observations differ strongly in character. Both of the cases presented below have been discussed by *Webster and Heymsfield* [2003] in more detail.

[29] Figure 5 illustrates the flight track of the WB57 on 28 July 2002. The aircraft, at nearly constant altitude flies through several locations with up to thousands of parts per million of ice (Figure 5a). The model is able to capture some of this variability. Note that for each observation, 27 model points varying in latitude, longitude and altitude around the observation are shown. Accompanying these events with high total water are small depletions of the isotopic species (Figure 5b), with δD near 0 per mil. This is

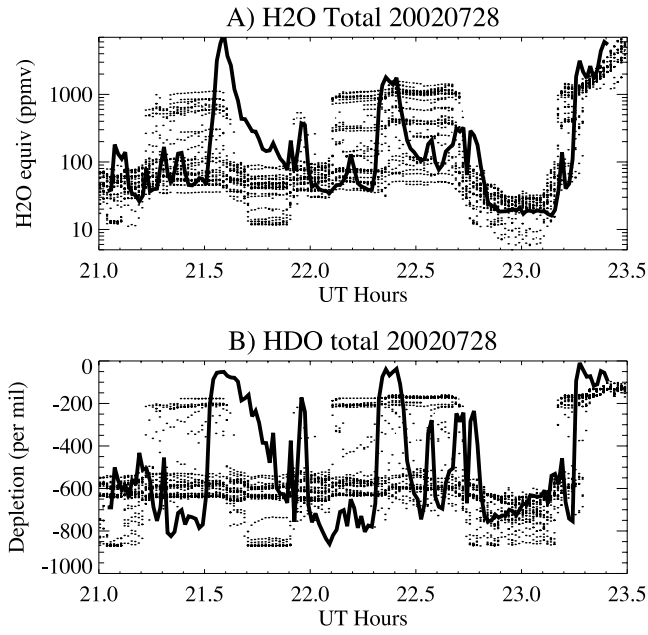

Figure 5. Observations (thick lines) and simulations (dots) along flight tracks (shown as a function of time in UTC hours) for the WB57 flight of 28 July 2002. (a) Total water from ALIAS in ppmv; (b) δD of total HDO (per mil).

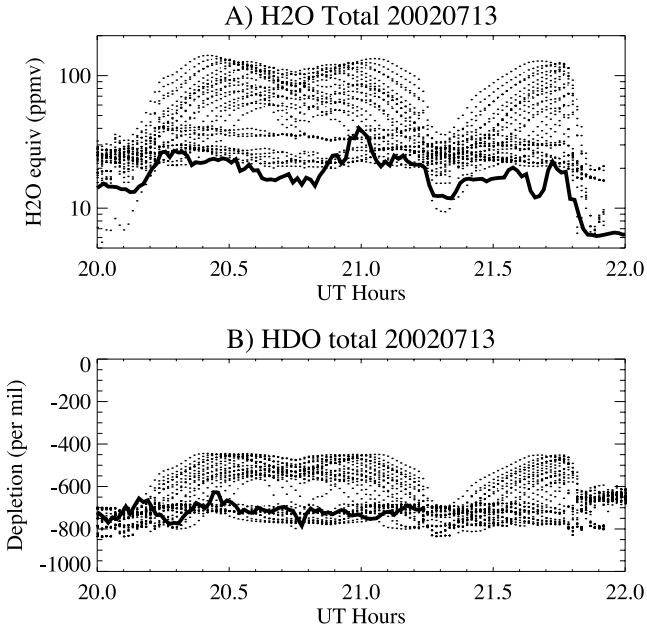

Figure 6. As in Figure 5 but for the WB57 flight of 13 July 2002.

especially evident during the passage through clouds at 21.6 UTC and 22.4 UTC. We note that the decay of the total water signal is due to the aircraft flying though a convective cloud, and then through its anvil, and is most likely not an instrument hysteresis effect. The model is able to capture this variability quite well. In examining the trajectories, these are locations in which air is undergoing rapid vertical ascent of several kilometers and large amounts of condensate are forming and spreading into the anvil. Note also that there is another convective event at about 23.2 UT, after water has dropped to 10–20 ppmv at 23.0 UT. Similar results are obtained for $H_2^{18}O$ (not shown).

[30] Figure 6 presents a different case from 13 July 2002 off the coast of Nicaragua when the WB57, while flying level in the upper troposphere at 15 km and 355 K potential temperature, encountered a cloud at 21.0 UTC. With ~15 ppmv of water vapor, the aircraft measured nearly 40 ppmv of total water (Figure 6a). Yet the isotopic composition of the total water did not change at all from the adjacent air (Figure 6b). The simulation captures this behavior as well. Note that the model also reproduces the distinction in air mass as the aircraft climbs at the end of this trace to 18 km at 22 UTC, and the water (total and vapor) declines rapidly to stratospheric values.

[31] The key point of Figures 5 and 6 is that the trajectories based on global analyses are able to capture the wide range of variability in total water observed from the aircraft. Convective events and cirrus cloud events are both properly represented. This large variation in total water (several orders of magnitude) also contains a large variation in isotopic ratio in the UT/LS region (Figure 3), and in the TTL (Figure 4) for a given total water mixing ratio.

3.3. Comparison to ALIAS $H_2^{18}O$

[32] We also analyze $H_2^{18}O$ in the model and compare it to observations. Figure 7 is similar to Figure 2 except showing the depletion of $H_2^{18}O$ in the observations and the simulation. The model is still able to broadly reproduce the phase space of the observations. Because the fractionation for $H_2^{18}O$ is not as large as for HDO, the atmosphere and model are not as depleted as for HDO. The model has a similarly broad range as the observations in the UT/LS. The model appears to have less depletion than the observations from 12 to 15 km. In both the model and observations, there are significant numbers of points that are more depleted than a simple Rayleigh curve would suggest. These points imply transport of air dehydrated at higher altitudes and/or at colder than observed temperatures assumed for this Raleigh distillation curve (a saturated adiabat starting at 300°K from the surface). These effects are minimized by plotting depletion versus the concentration of H_2O (not shown), but some anomalies persist, implying more complex mixing or measurement problems. We note that at high depletions (−200 per mil) observed $\delta^{18}O$ from ALIAS is generally larger than expected from the meteoric water line of HDO versus $H_2^{18}O$ and that ALIAS uncertainties are higher at lower total water amounts, as discussed in section 2.1. Such highly depleted points relative to a Rayleigh distillation curve are not seen in HDO. A plot for TTL air is similar between 13 and 17 km. The higher depletion is found typically in (chemically) "tropical" air.

[33] Discrepancies between the model and observed depletions for $H_2^{18}O$ are larger than for HDO. Because of the smaller depletion, and difficulty of ratioing spectral lines that differ in magnitude by a factor of five, the accuracy of the $\delta^{18}O$ measurements from ALIAS is less (uncertainty of ±50 per mil is 25–33%). We also note that the stratospheric values of $H_2^{18}O$ in the ALIAS observations of nearly −200 per mil are significantly more depleted than those observed by the FIRS instrument in the lower stratosphere of −130 per mil [*Johnson et al.*, 2001a], while the depletion of HDO is similar between the two instruments. However, FIRS did observe high (−200 per mil) depletions in limited samples of TTL air.

3.4. Comparison to ATMOS HDO

[34] Calculations were also performed for profiles of HDO taken from the ATMOS instrument on 11 November 1994, and the model compared to retrievals by *Kuang et al.* [2003]. ATMOS has 11 tropical profiles during a 3-day period, and of these five profiles extend down through the TTL. Because ATMOS is representing a large sampling volume (200 km horizontal), we have allowed ice condensate and vapor to come to equilibrium in these simulations.

[35] Figure 8 illustrates water vapor and isotopes from two of these profiles from ATMOS (dashed) and simulated with the model (solid). We show water vapor and ice in Figure 8a and ATMOS HDO compared to total HDO (vapor and ice) in the model in Figure 8b. While *Kuang et al.* [2003] and *Dessler and Sherwood* [2003] lumped all ATMOS profiles together to show "uniform depletion" of HDO in the TTL, we note that different profiles have a significantly different character to the depletion which our model is able to simulate. The profile at 96°E over the Indian Ocean has nearly uniform depletion down to 12 km, as does the model. The back trajectories 10 days prior originate in the stratosphere. However, in the Western Pacific at 140°E, the model and observations show enhanced depletion from 12 to 16 km, which is larger than the error indicated in

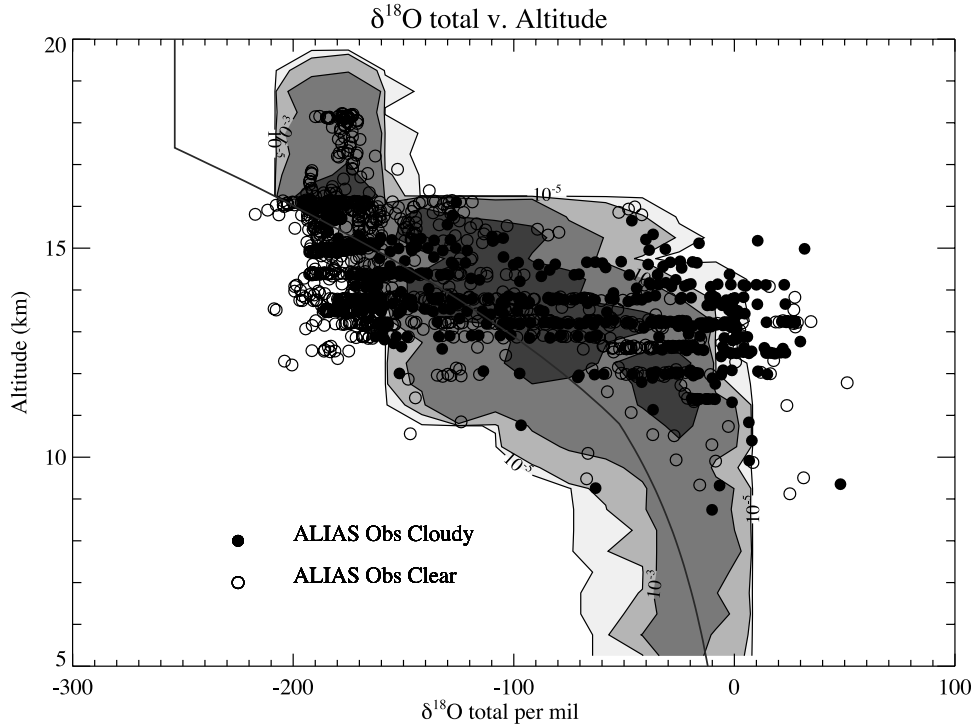

Figure 7. Depletion of $H_2^{18}O$ ($\delta^{18}O$) as a function of altitude. A PDF of model simulated results are shaded, and ALIAS observations are indicated for clear sky (open circles) and cloudy sky (closed circles). Cloudy sky is defined as total water greater than 120% of water vapor. A Rayleigh distillation curve from the surface is indicated as a black line. Contour intervals for the PDF are 10^{-5}, 10^{-4}, 10^{-3}, and 10^{-2}.

the observations. In this location and altitude range, the trajectories are influenced by convection, and begin near the surface 10 days prior. The large quantity of ice in this profile (up to 300 ppmv at 12–14 km) is not inconsistent with observations of ice from CRYSTAL-FACE, especially for convective events, and we presume that much of this ice would rapidly evaporate. The other three ATMOS profiles through the TTL have a similar character. A peak in depletion in the TTL depends on the influence of convection.

4. Discussion

[36] The analytic model does a good job of simulating isotopic depletion in the UT/LS, and the sharp gradient between the TTL and the stratosphere, which occurs in both the model and observations at the tropical tropopause, not the local tropopause. The ATMOS data in the TTL are consistent with the simulations of CRYSTAL-FACE data at the edge of the tropics, some of which has characteristics of the TTL. The key observation, proposed by *Moyer et al.* [1996] and noted by others [*Keith*, 2000; *Johnson et al.*, 2001b; *Webster and Heymsfield*, 2003], is that the atmosphere is often not near a Rayleigh curve, as a result of convective mixing, detrainment, and evaporation of ice. The analytic model indicates that this can be broadly explained with standard isotopic physics. We should expect a wide range of values of isotopic depletion in the UT/LS, and the depletion in the UT/LS and the TTL is not uniform. The degree of variability evidenced in the presence of tropical deep convection in total water (187 per mil from Table 1) is larger than previously observed in the UT/LS [*Ehhalt*, 1974] (70 per mil). This is to be expected because of the nature of deep convective transport of near surface water directly into the UT/LS region, as well as increased sensitivity and higher temporal sampling from ALIAS.

[37] Above the level of main convective outflow, slow ascent, dehydration, and concurrent fractionation can

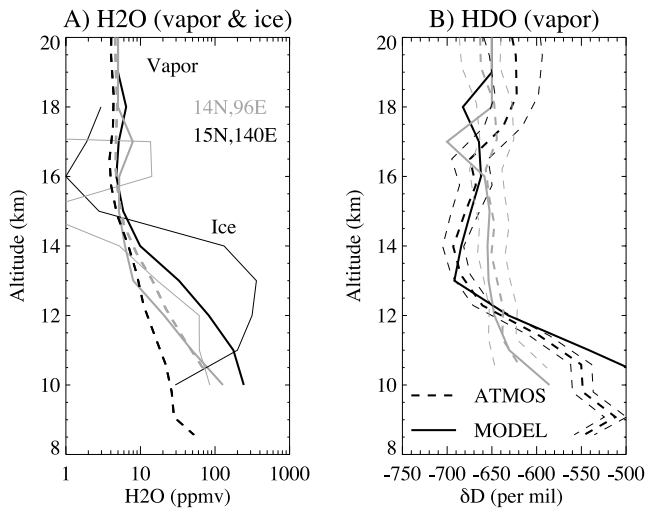

Figure 8. (a) Simulated (solid) and observed (dashed) water vapor (thick lines) and ice (thin lines–model only) for two ATMOS profiles on 11 November 1994 at 14°N, 96°E (gray) and 15°N, 140°E (black). (b) Corresponding HDO depletion (per mil) for the same profiles, with standard error for the ATMOS profile as thin dashed lines. Note that the simulated HDO depletion is for total water.

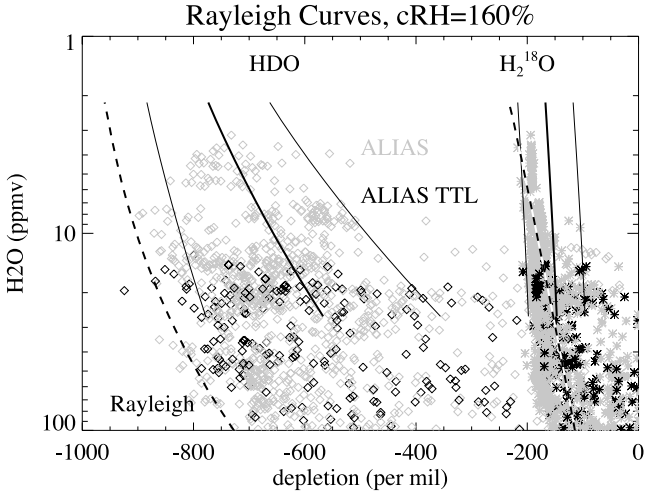

Figure 9. ALIAS isotope data for HDO (diamonds) and $H_2^{18}O$ (asterisks) overlaid with Rayleigh fractionation curves from the surface (dashed lines). Solid symbols are air characteristic of the TTL (as defined in the text), and gray symbols are all other points. Also shown are Rayleigh fractionation curves from the ALIAS observations 14–16 km average (thick solid lines) and 14–16 km average ±1 σ (thin solid lines) for HDO and $H_2^{18}O$.

explain the isotopic composition of the stratosphere. In Figure 9 the CRYSTAL-FACE observations of isotopic depletion for HDO and $H_2^{18}O$ are presented as a function of the water vapor mixing ratio for points with $[H_2O] < 100$ ppmv. Points with the chemical signature of the TTL (black) are separated from non-TTL air (gray). Also shown in Figure 9 are a series of Rayleigh curves at high supersaturation (160%) originating from the mean observed values in the TTL air from 14–16 km (−573 δD, −143 $\delta^{18}O$ from Table 1), and from ±1 σ from these values. High supersaturations are justified by recent observations of the upper troposphere and lower stratosphere [*Haag et al.*, 2003]. The curves bracket observed UT/LS and TTL values of H_2O and its isotopes. The key difference here between this estimate and those of previous authors is that we presume that fractionation up to the TTL occurs in convective clouds at low supersaturation where kinetic effects are less important and that dehydration outside of convective clouds occurs at high supersaturation. This is critical for matching both HDO and $H_2^{18}O$. Note the similar slopes between the supersaturated Rayleigh curve and $\delta^{18}O$ for $[H_2O] < 10$ ppmv. Dehydration under high supersaturations would also explain why the stratospheric values of $\delta^{18}O$ are closer to the observed minimum (Figure 7) than δD (Figure 2). Kinetic effects at high supersaturations reduce the fractionation of $H_2^{18}O$ much more than HDO. Note that it does appear as if the $H_2^{18}O$ observations are more depleted than the hypothetical line, but the slopes match well, which is the important point here. The larger uncertainty or slight systematic errors in the $H_2^{18}O$ data in this region may affect this result, though limited other observations corroborate the large $\delta^{18}O$ depletions observed.

[38] We further postulate, as have *Johnson et al.* [2001b] and *Dessler and Sherwood* [2003] that dilution rather than dehydration is also occurring. This dilution could be due to convective injection of dessicated air [*Sherwood*, 2000], but we think it is more likely to be due to isentropic mixing with aged stratospheric air. Extratropical lower stratospheric air has $[H_2O] \sim 5–6$ ppmv of H2O, $\delta D \sim -500$ [*Johnson et al.*, 2001a] and $[CH_4] \sim 1500$ ppbv. A tracer-tracer plot of δD or $\delta^{18}O$ versus $[CH_4]$ from the CRYSTAL FACE observations indicates $[CH_4] \sim 1600$ ppbv at the highest levels with $\delta D \sim -700$ and $\delta^{18}O \sim -180$. Maximum depletions occur for $[CH_4] \sim 1800–1700$ ppbv. It appears likely that some stratospheric air (potentially 1/3 by the methane concentrations) has also been mixed into the highest levels, and larger depletions are associated with near surface air brought up in convection.

5. Conclusions

[39] In situ and remotely sensed observations of isotopic water concentrations in the UT/LS can be reproduced with high fidelity using a simple analytic model along trajectories. The model reproduces the shape of the distribution, and the difference in shape between HDO and $H_2^{18}O$. The results are valid for regions which exhibit thermodynamic and chemical characteristics of the tropical tropopause layer.

[40] The results indicate that standard isotopic physics and kinetics can explain the observed isotopic distribution. The model can explain the variations in both the ATMOS and CRYSTAL-FACE observations. Most importantly, the tropical atmosphere is not a Rayleigh distillation process, due to the transport, detrainment, and evaporation of ice in anvils or above. The model is able to partially, but not fully, simulate this variability. For reproducing large-scale remotely sensed observations, unresolved mixing is required. The limitation of the model is due to its bulk nature and coarse transport, which does only implicitly simulates convective transport, and not the details of convective transport.

[41] The simulations and observations also indicate that slow ascent and horizontal transport from convective outflow and anvils is consistent with the isotopic concentration of the stratosphere. To explore the entry of air into the stratosphere, we have used the chemical signature of tropical air to filter extratropical from TTL air in a region which thermodynamically resembles the TTL in structure at the edge of the tropics. Simulations of ATMOS data in the TTL are consistent with the simulations of CRYSTAL-FACE data at the edge of the tropics.

[42] The key insight is that condensation processes in convection typically occur at low supersaturations, and kinetic effects are less important, allowing larger depletions of $H_2^{18}O$ in the TTL. Subsequent dehydration in thin cirrus clouds is likely to occur at high supersaturations, and kinetic effects significantly reduce the fractionation of $H_2^{18}O$. This hypothesis is consistent with the different shapes of the $\delta^{18}O$ and δD distributions in the TTL and stratosphere. Mixing with aged stratospheric air above the TTL may also modify isotopic concentrations by "dilution". Slow dehydration may also not be a Rayleigh process, and may not be efficient at fractionating air. There still remains some uncertainty between the existing observations of stratospheric $H_2^{18}O$ [*Webster and Heymsfield*, 2003], though the model still lies within the spread of the ALIAS observations. It would be especially valuable to continue to develop

and make measurements of $H_2^{18}O$ in the TTL and lower stratosphere.

[43] Given the importance of the convective influence, and possible in situ dehydration, we postulate that there are variations in the ambient isotopic depletion of HDO and $H_2^{18}O$ with (1) the presence or absence of convection in the UT/LS and (2) large-scale temperatures and the presence of cirrus clouds in the upper troposphere. Convection that overshoots its level of neutral buoyancy is likely to result in larger observed depletions. It is not possible at this time with only the CRYSTAL-FACE observations (given their variability and limited scale) to derive global budgets and constraints on water vapor isotopes, and further observations will be necessary in key regions to fix the relative importance of these various processes using isotopes.

[44] These simulations also serve as a caution to large-scale (global) models which seek to simulate the isotopic concentration of water vapor in the upper troposphere and lower stratosphere. Significant reevaporation and ice detrainment, as well as supersaturation for ice clouds, may be necessary for bulk formulations to do a good job of simulating the isotopic composition of stratospheric water vapor.

[45] **Acknowledgments.** AG would like to sincerely thank D. H. Ehhalt, Z. Kuang, and D. G. Johnson for the liberal use of their data, and their diligence and foresight for its careful production. All credit goes to them, and all misuse falls upon me. We thank E. Weinstock for the use of the Harvard water data. We would also like to thank D. H. Ehhalt, W. R. Randel, and A. J. Heymsfield for discussions. This research at the National Center for Atmospheric Research (NCAR) was supported by a NASA Atmospheric Chemistry Modeling and Analysis Program grant (ACMAP2000-0000-0086). NCAR is supported by the National Science Foundation.

References

Baumgardner, D., H. Jonsson, W. Dawson, D. O'Connor, and R. Newton (2001), The cloud, aerosol and precipitation spectrometer (CAPS): A new instrument for cloud investigations, *Atmos. Res.*, *59–60*, 251–264.

Brewer, A. W. (1949), Evidence for a world circulation provided by the measurements of helium and water vapor distribution in the stratosphere, *Q. J. R. Meteorol. Soc.*, *75*, 351–363.

Cappa, C. D., M. B. Hendricks, D. J. DePaolo, and R. C. Cohen (2003), Isotopic fractionation of water during evaporation, *J. Geophys. Res.*, *108*(D16), 4525, doi:10.1029/2003JD003597.

Dessler, A. E., and S. C. Sherwood (2003), A model of HDO in the tropical tropopause layer, *Atmos. Chem. Phys.*, *3*, 2173–2181.

Ehhalt, D. H. (1974), Vertical profiles of HDO, HTO and H_2O in the troposphere, *Tech. Note STR-100*, Natl. Cent. for Atmos. Res., Boulder, Colo.

Folkins, I., M. Loewenstein, J. Podolske, S. J. Oltmans, and M. Proffitt (1999), A barrier to vertical mixing at 14 km in the tropics: Evidence from ozonesondes and aircraft measurements, *J. Geophys. Res.*, *104*(D18), 22,095–22,102.

Gettelman, A., and P. M. F. Forster (2002), A climatology of the tropical tropopause layer, *J. Meteorol. Soc. Jpn.*, *80*(4B), 911–924.

Gettelman, A., W. J. Randel, F. Wu, and S. T. Massie (2002), Transport of water vapor in the tropical tropopause layer, *Geophys. Res. Lett.*, *29*(1), 1009, doi:10.1029/2001GL013818.

Gettelman, A., P. M. F. Forster, M. Fujuwara, Q. Fu, H. Vomel, L. K. Gohar, C. Johanson, and M. Ammeraman (2004a), The radiation balance of the tropical tropopause layer, *J. Geophys. Res.*, *109*, D07103, doi:10.1029/2003JD004190.

Gettelman, A., D. E. Kinnison, T. J. Dunkerton, and G. P. Brasseur (2004b), The impact of monsoon circulations on the upper troposphere and lower stratosphere, *J. Geophys. Res.*, *109*, D22101, doi:10.1029/2004JD004878.

Haag, W., B. Karcher, J. Strom, A. Minikin, U. Lohmann, J. Ovarlez, and A. Stohl (2003), Freezing thresholds and cirrus cloud formation mechanisms inferred from in situ measurements of relative humidity, *Atmos. Chem. Phys.*, *3*, 1791–1806.

Heymsfield, A. J. (2003), Properties of tropical and midlatitude ice clouds particle ensembles. Part II: Applications for mesoscale and climate models, *J. Atmos. Sci.*, *60*, 2592–2611.

Holton, J. R., P. H. Haynes, A. R. Douglass, R. B. Rood, and L. Pfister (1995), Stratosphere–troposphere exchange, *Rev. Geophys.*, *33*(4), 403–439.

Hoor, P., C. Gurk, D. Brunner, M. Hegglin, H. Wernli, and H. Fischer (2004), Seasonality and extent of extratropical TST derived from in-situ CO measurements during SPURT, *Atmos. Chem. Phys. Disc.*, *4*, 1691–1726.

Johnson, D. G., K. W. Jucks, W. A. Taub, and K. V. Chance (2001a), Isotopic composition of stratospheric water vapor: Measurements and photochemistry, *J. Geophys. Res.*, *106*(D11), 12,211–12,227.

Johnson, D. G., K. W. Jucks, W. A. Taub, and K. V. Chance (2001b), Isotopic composition of stratospheric water vapor: Implications for transport, *J. Geophys. Res.*, *106*(D11), 12,219–12,226.

Jouzel, J., and L. Merlivat (1984), Deuterium and oxygen 18 in precipitation: Modeling of the isotopic effects during snow formation, *J. Geophys. Res.*, *89*(D7), 11,749–11,757.

Keith, D. W. (2000), Stratosphere-troposphere exchange: Inferences from the isotopic composition of water vapor, *J. Geophys. Res.*, *105*(D12), 15,167–15,173.

Kuang, Z., G. C. Toon, P. O. Wennberg, and Y. L. Yung (2003), Measured HDO/H_2O ratios across the tropical tropopause, *Geophys. Res. Lett.*, *30*(7), 1372, doi:10.1029/2003GL017023.

McCarthy, M. C., et al. (2004), The hydrogen isotopic composition of water vapor entering the stratosphere inferred from high precision measurements of δD-CH_4 and δD-H_2, *J. Geophys. Res.*, *109*, D07304, doi:10.1029/2003JD004003.

Moyer, E. J., F. W. Irion, Y. L. Yung, and M. R. Gunson (1996), ATMOS stratospheric deuterated water and implications for troposphere-stratosphere transport, *Geophys. Res. Lett.*, *23*(17), 2385–2388.

Randel, W. J., F. Wu, and W. R. Rios (2003), Thermal variability of the tropical tropopause region derived from GPS/MET observations, *J. Geophys. Res.*, *108*(D1), 4024, doi:10.1029/2002JD002595.

Ridal, M. (2002), Isotopic ratios of water vapor and methane in the stratosphere: Comparison between ATMOS measurements and a one-dimensional model, *J. Geophys. Res.*, *107*(D16), 4285, doi:10.1029/2001JD000708.

Rosenlof, K. H. (2003), How water enters the stratosphere, *Science*, *302*, 1691–1692.

Sherwood, S. C. (2000), A stratospheric "drain" over the maritime continent, *Geophys. Res. Lett.*, *27*(5), 677–680.

Stratospheric Processes and their Role in Climate (SPARC) (2000), Assessment of water vapor in the upper troposphere and lower stratosphere, Stratospheric Processes and Their Role In Climate, *Rep. WMO/TD-1043*, World Meteorol. Org., Geneva.

Webster, C. R., and A. J. Heymsfield (2003), Water isotope ratios D/H, $^{18}O/^{16}O$, $^{17}O/^{16}O$ in and out of clouds map dehydration pathways, *Science*, *302*, 1742–1745.

Weinstock, E. M., et al. (1994), New fast response photofragment fluorescence hygrometer for use on the NASA ER-2 and the Perseus remotely piloted aircraft, *Rev. Sci. Instrum.*, *65*, 3544–3554.

A. Gettelman, National Center for Atmospheric Research, Box 3000, Boulder, CO 80307-3000, USA. (andrew@ucar.edu)

C. R. Webster, Earth and Space Sciences Division, Jet Propulsion Laboratory, California Institute of Technology, Pasadena, CA, USA.